Since January 2020 Elsevier has created a COVID-19 resource centre with free information in English and Mandarin on the novel coronavirus COVID-19. The COVID-19 resource centre is hosted on Elsevier Connect, the company's public news and information website.

Journal of the Taiwan Institute of Chemical Engineers 115 (2020) 251–265

Contents lists available at ScienceDirect

Journal of the Taiwan Institute of Chemical Engineers

journal homepage: www.elsevier.com/locate/jtice

Electrochemical-kinetics, MD-simulation and multi-input single-output (MISO) modeling using adaptive neuro-fuzzy inference system (ANFIS) prediction for dexamethasone drug as eco-friendly corrosion inhibitor for mild steel in 2 M HCl electrolyte

Valentine Chikaodili Anadebe[a,*], Okechukwu Dominic Onukwuli[b], Fidelis Ebunta Abeng[c], Nkechinyere Amaka Okafor[a], Joseph Okechukwu Ezeugo[d], Chukwunonso Chukwuzuloke Okoye[b]

[a] Department of Chemical Engineering, Federal University Ndufu Alike, Ebonyi state, Nigeria
[b] Department of Chemical Engineering, Nnamdi Azikwe University, Anambra state, Nigeria
[c] Material & Electrochemistry Unit, Department of Chemistry, Cross River University of Technology Nigeria
[d] Department of Chemical Eng. Chukwuemeka Odumegwu Ojukwu University, Anambra state, Nigeria

ARTICLE INFO

Article History:
Received 4 August 2020
Revised 4 October 2020
Accepted 5 October 2020
Available online 21 October 2020

Keywords:
Acid corrosion
ANFIS
EIS
Dexamethasone drug
Mild steel
MD-simulation

ABSTRACT

In this research, the effect of Dexamethasone drug (DM) on mild steel corrosion in 2 M HCl was analyzed using weight loss, potentiodynamic polarization, electrochemical impedance spectroscopy (EIS) and MD-simulation. In addition, Fourier transform infrared spectra (FTIR), scanning electron microscopy (SEM), Energy dispersive x-ray spectroscopy (EDX), and atomic force microscopy (AFM) were employed to inspect the mild steel surface in the blank and inhibited medium. For the optimization tool, adaptive neuro-fuzzy inference system (ANFIS) model was developed to predict the inhibition efficiency. The experimental data was categorized into two different sections for training and testing the ANFIS model. The developed model aimed to evaluate the fitness between the experimental and predicted values. From the results generated, optimum value (IE%) of DM was recorded as 80%, 81% and 83% at concentration of 0.4 g/L for weight loss, EIS and PDP respectively. Potentiodynamic polarization results reveal that Dexamethasone functions as a mixed-type inhibitor, whereas studies of EIS show that the inhibition mechanism is by the transfer of charges. Mild steel surface examination confirmed the presence of a protective adsorbed film on the mild steel surface. Thermodynamic parameters obtained imply that Dexamethasone is adsorbed on the steel surface by a physiochemical process and obeys Langmuir adsorption isotherm. Also the MD-simulation results evidenced that DM forms a metallic surface adsorbed film on the steel surface. From the ANFIS model, the sensitivity analysis shows that time and inhibitor concentration were the most important input variable while other input variables could not be neglected. ANFIS model coefficient of determination (R^2 0.993) was found between the observed and predicted values. ANFIS model gave optimum prediction (80%) with high degree accuracy and robustness.

The outcomes of this investigation provide more information, simulation, and prediction about inhibition of metal corrosion.

1. Introduction

The destruction (or deterioration) of a metal and unwanted chemical or electrochemical attack by its environment starting at the surface is called corrosion. Corrosion can damage pipelines, bridges, public buildings, water and wastewater systems and if neglected can be catastrophic [1]. It is one of the most severe oil and gas industrial problems. Metal corrosion has caused huge economic losses in many industries, involving billions of dollars each year. The international corrosion prevention application and economic measure estimated global corrosion cost to 1–5% of an industrialized country's gross national product [2]. They suggested that implementing corrosion prevention could lead to global savings of 15–35%. Control measures or procedures therefore need to be introduced to minimize or prevent corrosion thereby prolonging the life span of metals [3]. Different methods for protection of metals from corrosion were suggested and implemented. One of these methods is the use of corrosion

* Corresponding author.
E-mail address: anadebe.valentine@funai.edu.ng (V.C. Anadebe).

https://doi.org/10.1016/j.jtice.2020.10.004
1876-1070/

inhibitor which is one of the best corrosion control method. Corrosion inhibitors have been known to be an effective and simpler means of preventing corrosion [4–6].

A corrosion inhibitor is a chemical substance or a combination of substances that when applied to a corrosive environment in very limited amounts effectively reduce or inhibit corrosion without interacting significantly with the environmental components [7]. Corrosion inhibitors have found applications in different industries like oil and gas, chemical industries, heavy production processing and water treatment plants [8]. Corrosion inhibitors may be categorized as organic or inorganic compounds and can typically dissolved in corrosive environments. It should be noted that most organic and synthetic inhibitors are not biocompatible and economically cost effective. For this reason, these types of inhibitors became useless and outdated and current studies are directed towards application of inexhaustible, biocompatible, and nontoxic inhibitors [3].The growing understanding of health, safety and environment has drawn researcher's attention to develop very powerful and productive environmentally friendly inhibitors. Typical examples of such inhibitors that are environmentally friendly are fast green [9]. Fast green molecules have an aromatic ring with electroactive nitrogen and oxygen atoms while the Dexamethasone molecule has electroactive oxygen and carbon atoms with aromatic rings (rich electrons). Fig. 1 displays the molecular structure of the studied compound, these compounds are drug based and are adsorbed on the metal surface thereby blocking the active site of the metal resulting to decrease in the rate of corrosion and thus increasing the inhibition efficiency [10,11].

In the field of corrosion many researchers have agreed that drugs are inhibitors of corrosion, and can favorably compete with the natural products [12,13].

There are a large number of reports on the use of drug based compounds as corrosion inhibitor for metal corrosion prevention in aggressive environment. The impact of tobramycin drug on carbon steel in 2 M HCl solution was examined by Abeng et al. [14]. They reported the inhibition efficiency of 80% using 500 ppm inhibitor. The electrochemical and quantum chemical studies on adsorption of nifedipine as corrosion inhibitor at API 5LX-52 steel/ HCl acid interface was investigated by Ikpi and Abeng [15]. They found that nifepidine drug performed as a mixed type corrosion inhibitor and a maximum inhibition efficiency of 88.5% was determined with a 500 ppm solution of inhibitor. The adsorption process of the drug on API 5LX-52 steel was successfully interpreted by the Langmuir model. Also the quantum chemical studies revealed the feasible adsorption areas of the nifedipine molecule. El-Haddad et al. [16] studied the carbon steel corrosion rate in acidic medium containing cephapirin drug. They showed that the corrosion inhibitor molecules adsorption on the steel surface resulted in achievement of inhibition efficiency of 83% at 600 ppm and temperature of 303 K. The inhibitory action of expired asthalin drug on the corrosion of mild steel in acidic media was studied by Geethamani et al. [17]. They found that inhibition efficiency increases with the increase of inhibitor concentration, time and temperature. A mixed mode of inhibition mechanism was proposed for the effect of asthalin drug. The highest inhibition efficiency (73.68%) was retrieved for an inhibitor concentration of 9.0% v/v, also the adsorption thermodynamic was best interpreted by the Langmuir isotherm. Sumayah et al. [18] predicted the suitability of bronopol as a corrosion inhibitor for aluminum metal in 0.5 M HCl using weight loss data combined with the electrochemical measurement. They found that bronopol exhibits a maximum of 93.89% inhibition efficiency at 4000 ppm. Also the adsorption of bronopol on aluminum surface tends to obey Langmuir isotherm. The polarization measurement revealed bronopol to be a mixed sort inhibitor. Abdallah et al. [19] evaluates the performance of tramadol drug as a safe inhibitor for aluminum corrosion in 1 M HCl solution. They found that inhibition efficiency increases with the increase inhibitor concentration. Tramadol drug is a mixed inhibitor mainly anodic. They reported inhibition efficiency of 98% at temperature of 25 °C and inhibitor concentration of 500 ppm. Electrochemical and quantum chemical studies on corrosion inhibition performance of 2,2′-(2-Hydroxyethylimino)bis[N-(alphaalpha-dimethylphenethyl)-N-methylacetamide] on mild steel corrosion in 1 M HCl solution was investigated by Iman et al. [20]. In their study, inhibition efficiency increased with an increase in inhibitor concentration. Maximum inhibition efficiency of 95% at 200 ppm was achieved. Polarization studies revealed that the drug molecule was a mixed type inhibitor.

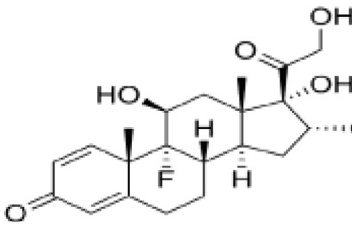

Fig. 1. Molecular structure of dexamethasone.

The above literature analysis highlights the importance of identifying effective corrosion inhibitors for mild steel in order to increase safety, less maintenance costs and restricts the use of imported chemical inhibitors when it is adopted, especially, in the industries, for flow systems or chemical plants experiencing severe acidic conditions [21]. For the purpose of marketability of new discovered inhibitors, the latter should be closely examined by low cost, availability and near-to-zero environmental impact. Following this direction, this present work proposes the application of a novel drug (Dexamethasone) as a potential additive for mitigation of corrosion. Dexamethasone is a synthetic corticosteroid and derivative of cortisol. It is whitish in nature, odorless and a crystalline powder with molecular formula $C_{22}H_{29}FO_5$, it helps in treatment of severe conditions like allergies and some common diseases. Dexamethasone is much cheaper and easy to procure. These outstanding characteristics have necessitated an ongoing research with a major breakthrough on the use of Dexamethasone in treatment of COVID 19.

In Chemical Engineering discipline to be precise, soft computing models and simulations have been enormously used in promising areas of research [22–26]. Modeling, simulation and solving complex nonlinear problems is one of the breakthrough applications of artificial intelligence like fuzzy inference programs, ASPEN HYSIS, artificial neural network (ANN), Genetic algorithm (GA) and RSM models. Some well-respected scientists with similar research interest have used different soft computing and modeling techniques and positive results were generated [27–34], although the application of ANFIS is very scarce in this area. Thus, multi objective interest in this current research is to examine the interfacial adsorption and active sites of Dexamethasone drug at atomic and molecular rates using MD simulation concept, secondly for the first time, to use ANFIS model to predict the inhibition efficiency and to test the model application to pin point nonlinear complex interaction between independent variable and expected response.

2. Materials and method

2.1. Materials

Corrosion studies were performed on mild steel of compositions Mn (0.13%), P (0.22%), Si (0.05%), S (0.12%), C (0.24%), Cr (0.02%), Ni (0.07%), and Fe (99.15%). Prior to corrosion studies, the mild steel was mechanically cut ($5 \times 4 \times 0.1$ cm). Each coupon was abraded using 220, 600 and 800 emery papers to obtain a smooth / uniform surface area. The coupons were further degreased with acetone, rinsed with deionized water to remove debris and dried in warm air. This is in line with technique of previous report [35].

2.2. Methods

2.2.1. Preparation of 2 M HCl and inhibitor

171.82 HCl (37 wt%, specific gravity of 1.18) was added to 800 ml of distilled water in 1 liter measuring cylinder. The solution was made up to 1 liter with addition of distilled water. Dexamethasone drug (DM) used as inhibitor was obtained from G & I Pharmaceutical Company, Calabar, Nigeria without further purification. 5 g of ground Dexamethasone drug was dissolved in 1 liter of 2 M HCl solution. From the stock solution (5 g/L), Dexamethasone drug test solutions were prepared at concentrations of 0.1, 0.2, 0.3, 0.4 and 0.5 g/L respectively [36].

2.2.2. Weight loss measurements

We performed weight loss experiment at varying temperatures. Test coupons in triplicates were suspended freely in glass reaction vessels containing 200 ml of test solution (2 M HCl) without and with varying inhibitor concentrations. At the appropriate time, the mild steel samples were taken out, immersed in acetone, scrubbed with a bristle brush under running water, and dried in warm air before reweighing. The weight loss was calculated in grammes as the difference between the initial weight and the weight after the removal of the corrosion product. The experimental readings were recorded. The weight loss (Δw), corrosion rate (CR), inhibition efficiency (IE), and degree of surface coverage (θ) were calculated using Eqs. (1–4) [35].

$$\Delta w = w_i - w_f \tag{1}$$

$$C_R = \frac{w_{bl} - w_{inh}}{Area(m^2)x(time)day} \tag{2}$$

$$IE\% = \frac{w_{bl} - w_{inh}}{w_{bl}} \text{x} 100 \tag{3}$$

$$\theta = \frac{w_{bl} - w_{inh}}{w_{bl}} \tag{4}$$

where w_1 and w_2 are initial and final weight loss of mild steel respectively.CR_{blank} and $CR_{inhibitor}$ are the corrosion rate of mild steel in absence and presence of inhibitor. 'A' is the total area of the mild steel sample and't' is the time of immersion.

2.2.3. Electrochemical measurements

Electrochemical measurement was performed in 2 M HCl solution in absence and presence of different concentrations of inhibitor at 30 °C. Within the context of this study two components of epoxy resin were used to mount the mild steel in a PVC holder connected with a copper wire forming a working electrode with a surface area of 1cm^2. The electrochemical study was done using a VERSASTAT 400 full set DC Voltammetry and a Potentiodynamic/ Galvanostat corrosion system with E-chem software for polarization study. The procedures for the electrochemical measurement are as follows: electrochemical cell assembly comprising of mild steel known as working electrode, 1 cm × 1 cm platinum foil used as counter electrode, and the saturated calomel electrode representing the reference electrode [37]. The entire electrochemical measurement was performed in a 200 ml glass filled with the test solution. Prior to each experimental measurement the test solution was stabilize at 100 s. EIS measurement was carried out over the frequency range of 100 KHz to 10 MHz with signal amplitude of 5 mV. Zsimpwin 3.0 software was used to analyze the impedance data. Potentiodynamic polarization measurements were performed at the scan rate of 0.33 mV/s. The potential range was ± 250 mV versus corrosion potential. The experiment was run in triplicates to scrutinize and justify the reproducibility of average values obtained for further statistical analysis. The following Equations were used for the calculation of inhibition efficiency.

$$IE\% = 1 - \frac{R_{ct}(bl)}{R_{ct}(inh)} \text{X} 100 \tag{5}$$

$$IE\% = \frac{i_{corr(bl)} - i_{corr(inh)}}{i_{corr(bl)}} \text{X} \frac{100}{1} \tag{6}$$

Where $R_{ct(bl)}$ and $R_{ct(inh)}$ represent the charge transfer resistance in uninhibited and inhibited solution and corrosion current densities in uninhibited and inhibited solution represented as $i_{corr(bl)}$ and $i_{corr(inh)}$ respectively.

2.3. Molecular dynamics and simulation

The quantum chemical calculations and MD-simulation were performed using the DFT electronic structure programs Forcite and $DMol^3$ as embedded in the materials studio 4.0 software. The electronic parameters for the simulation include unrestricted spin polarization using DND basis set and perdew-Wang (PW) local correlation density functional. The Fe slab for the simulations was cleaved along the (110) plane. The calculations were performed in a 12 × 10 super cell using a Compass force field (condensed phase optimized molecular potential simulation studies) and the Smart algorithm with NVE (micro canonical) ensemble, a time step of 1 fs and simulation time of 5 ps. The temperature was fixed at 303 K. The system was quenched automatically at intervals of 250 steps.

2.4. MISO modeling with adaptive-neuro fuzzy inference system (ANFIS)

ANFIS is a unique optimization tool as it has the capability to model and scrutinize stochastic values with high level of accuracy. ANFIS modeling requires data for independent variables (MI) and dependent variable (SO). The coding or network program focuses on Takagi-Sugeno fuzzy inference system [23]. ANFIS program uses back-propagation and least square evaluation for prediction of membership function. The adaptive network normally consists of nodes and directional links, which are the connectors of the node. The nodes are purely adaptive because they depend on the node parameters, and during learning; these parameters are changed based on the learning rules with a target on minimizing a prescribed error measure. The Takagi-Sugeno program is used in ANFIS where every rule's output is constant. The ANFIS rule is categorize into two as given below.

$$\text{First rule}: -\text{if } x \text{ is } A_1 \text{ and } y \text{ is } B_1; \text{then } f = p_1 x + q_1 y + r_1 \tag{7}$$

$$\text{Second rule}: -\text{if } x \text{ is } A_2 \text{ and } y \text{ is } B_2; \text{then } f = p_2 x + q_2 y + r_2 \tag{8}$$

:A_1,A_2,B_1andB_2 are nonlinear numbers whilep_1,p_2,q_1,q_2 and $r_1$andr_2 are linear numbers.

A statistical criterion $R^2$was employed for predicting the model's order. R^2evaluates the conformity (fitness) between the experimental and predicted data set using the following equation:

$$R^2 = 1 - \frac{\sum_{i=1}^{m} \left(x_{i,e} - x_{i,P}\right)^2}{\sum_{i=1}^{m} \left(x_{i,P} - x_{e,a}\right)^2} \tag{9}$$

Prior to ANFIS analysis and prediction, 14 runs of experiment were considered. The experimental data were normalized. Normalization is refers to changing the experimental data to values between 0 and 1. It is pertinent to normalize such data to ensure error free (zero) on completion of system analysis. The Z-score normalization method through mean and standard deviation of training data for normalizing the input values was done using the following equation

$$Norm(n) = \frac{(x_i - \mu_i)}{\sigma_i} \tag{10}$$

Where$x_i$is input data set, μ_i is mean of$x_i\sigma_i$ standard deviation of $x_iNorm(n)$ is normalized variablexas input to ANFIS environment.

2.5. Surface film analysis of mild steel and FTIR studies

The mild steel coupons were immersed in test solution at 303 K for duration of one day. The coupons were then taken out and dried after one day. The nature of the film formed on the metal surface was analyzed by Fourier transform infrared (FTIR), Scanning electron microscope in combination of energy dispersive x-ray SEM-EDX, For the SEM analysis, the electron beam acceleration takes place through the voltage system 15 kV. The electron beam gets narrowed after passing through the apertures and electromagnetic lens. Afterwards the beam scans the metal surface with the help of scan coils. The images are generated after production of SEM types of signals from the area of beam and specimen interaction. In addition, atomic force microscope (AFM) was used to estimate the mean roughness (Ra) on mild steel specimens [38].

3. Results and discussion

3.1. Weight loss measurement

3.1.1. Effect of immersion time

When characterizing corrosion inhibitor, time is a standout factor used in the determination of the inhibitor film stability and the rate at which inhibitor adsorption occur. The periods of immersion varied between 1 and 5 h. The findings are shown in Table 1, which indicates the impact of time on the inhibition performance of Dexamethasone drug. The inhibition efficiency systematically increased from the early immersion period, which was 2–4 h. This was due to the inhibitor's rapid adsorption to the mild steel surface due to the maximum number of active inhibitor molecules available for the surface coating. The inhibition efficiency was observed to decline slightly after 4 h of immersion, this could be associated with more dissolution energy effect acquire by the corrosive agents within the aggressive environment [39].

3.1.2. Effect of dexamethasone drug concentration

The dissolution of mild steel in acidic media over a period of five hours was demonstrated in the form of electrochemical reactions [40]. The dexamethasone drug concentration varied with inhibition efficiency is shown in Table 1. With the increase in dexamethasone concentration, the inhibition efficiency expedite due to the existence of vast amounts of adsorption sites caused by other concentrations of macromolecules. Calculation of the inhibition efficiencies from corrosion rates was shown by Eqs. (2) and (3) whereas surface coverage was calculated by Eq. (4). The optimum inhibition efficiency of dexamethasone was recorded as 80.17% at the concentration of 0.4 g/L. This is attributed to the availability of C and O in the drug compound that participates as active centers and electrostatic forces in the inhibitory action between dexamethasone and the steel surface. The active functional groups which are carbonyl in the studied compound and other groups interact with the surface of MS by electron donation to the d-orbital of Fe, thus enabling the adsorption of Dexamethasone to the surface of the mild steel [41–42].

3.1.3. Effect of temperature

Weight loss experiments were also used to test temperature effects on mild steel corrosion with the aid of corrosion inhibitor. The findings are listed in Table 1. The findings were used to quantify metal dissolution activation energy and Gibbs energy of inhibitor adsorption onto the mild steel surface. The inhibition efficiency was observed to increase rapidly at mild temperature increase and gradually decline after 333 K. The reduction in the inhibition efficiency at 343 K demonstrated Dexamethasone's instability when it is exposed to higher temperatures, which implies that Dexamethasone adsorption onto MS surface was a process of exothermia, heat is released during adsorption. In keeping with the theory of Le Chatelier when the reaction that occurs is exothermic, the temperature rise will induce the reverse of the reaction. The same is true of endothermic reactions as well [43]. Dexamethasone was found to function better at low to medium temperatures than at higher temperatures. Also, the desorption of adsorbed inhibitor molecules due to increased solution agitation by higher rates of hydrogen gas evolution at elevated temperature is possible and may cause the ability of the inhibitor to be adsorbed on the mild steel surface to reduce [44].

3.2. Activation energy, heat of adsorption and adsorption isotherm studies

E_a andQ_{ads}in 2 M HCl with Dexamethasone for mild steel protection are shown in Table 2. The measured$E_a$value for the inhibited solution with Dexamethasone ranges from 6.5437 to 21.7149 kJmol^{-1} in the presence of 0.1 and 0.3 g/L^{-1} inhibitor concentrations, while the activation energies range from 9.1619 to 16.4986 kJmol^{-1} in the 0.2 and 0.5 g/L^{-1} inhibitor concentrations. This work shows that the inhibited partial reaction of mild steel is due to the adsorption of the film layer on the metal surface. This is due to the nature of the studied heterocyclic compounds which shield the metal from further

Table 1
Effect of independent variables (time, IC, temperature) and the expected responses.

Time	W_o (g)	CR_o (mg/cm^{-2}h^{-1})	W_1 (g)	CR_1 (mg/cm^{-2}h^{-1})	IE (%)	ϴ
1 hr.	0.10	11.11	0.07	7.778	30.00	0.3000
2	0.18	10.00	0.09	5.000	50.00	0.5000
3	0.26	9.63	0.10	3.704	61.54	0.6154
4	0.41	11.39	0.11	3.056	80.17	0.8017
5	0.42	9.333	0.13	2.889	69.05	0.6905
Effect of Dexamethasone drug (inhibitor concentration)						
0.0 g/L^{-1}	0.41	11.39	–	–	–	–
0.1			0.31	8.611	24.39	0.2439
0.2			0.22	6.111	46.34	0.4634
0.3			0.18	5.000	56.10	0.5610
0.4			0.11	3.056	80.17	0.8017
0.5			0.12	3.333	70.73	0.7073
Effect of Temperature						
303 K	0.09	2.500	0.07	1.944	22.22	0.2222
313	0.17	4.722	0.09	2.500	47.06	0.4706
323	0.28	7.778	0.12	3.333	57.14	0.5714
333	0.41	11.39	0.11	3.056	80.17	0.8017
343	0.42	11.67	0.13	7.778	69.05	0.6905

Table 2
Activation energy, heat of adsorption and adsorption isotherm studies.

Inhibitor	E_a(KJ/mol)	Q_{ads}(KJ/mol)
0.1 g/L^{-1}	6.54	−2.83
0.2	9.16	−3.96
0.3	21.71	−13.41
0.4	17.86	−7.77
0.5	16.49	−7.14
Langmuir model parameters		
Log C	Log (C/θ) 323 K	Log (C/θ) 333 K
−1	−0.38721	−0.37676
−0.69897	−0.36493	−0.35449
−0.52288	−0.27184	−0.24204
−0.39794	−0.26227	−0.25182
−0.30103	−0.15063	−0.14019

dissolution [27]. In general,Q_{ads}negative values imply that Dexamethasone molecules' surface attachment was exothermic and spontaneous. In same vain the interaction of adsorbed molecules with the metal surface can be explained by various adsorption models. The essential step of the adsorption process of Dexamethasone molecule onto the mild steel surface is shown in Eq. (11), where (θ) is the surface coverage which was calculated from weight loss [45]. As revealed by the plot of log $\frac{C}{\theta}$ as a function of log C indicates a linear graph [46], with a mathematical model of slope values 0.311 to 0.3149 and intercepts 0.0895 to 0.1057 respectively. The regression factor (R^2) ranges from 0.929 to 0.930.During the analysis, adsorption model from Langmuir was tested and the model offered the best fit as shown in Fig. 2 and was used for calculating the free energy of adsorption according to Eq. (12).

$$\frac{C}{\theta} = \frac{1}{K_{ads}} + C \tag{11}$$

$$\Delta G_{ads} = -2.303RT \quad \log 55.5K_{ads} \tag{12}$$

where C is the concentration of inhibitor, R, T and$K_{ads}$is the molar gas constant, absolute temperature and equilibrium constant. The free threshold value for free energy of adsorption is − 40 kJ/mole which is more than the free energy of the present study 34.2 kJ/mole reflecting physical adsorption mechanism of the corrosion reaction [47].

3.3. Electrochemical measurements

Electro-kinetics and phenomenal nature of the electrochemical practice concerned in the corrosion and corrosion inhibition of mild steel in 2 M HCl solution was appreciated by electrochemical impedance spectroscopy (EIS). The EIS study was carried out in the uninhibited and inhibited solution. The spectra impedance present in 2 M HCl solution at 303 K are shown in Fig. 3a-3c as nyquist, bode phase angle and bode modulus plots accordingly. The blank was used as a reference point in comparing the results with that of the inhibited solution shown in Fig. 3a. The spectra exhibited an imperfect semicircle with double hump nature throughout the frequency study [35]. In the Nyquist impedance spectra, the solution resistance (*Rs*) represent the high frequency intercept with the real axis and charge transfer resistance (*Rct*) is the low frequency intercept with the real axis. The data for the impedance were fitted with circuit model shown as an inset in Fig. 3a. The model consists of C_{dl} and*Rct* representing the impedance effect due to the corrosion product species from the blank, fractal geometry, electrode geometry and porosity as describe by Eq. (13) [48].

$$Z_{CPE} = Q^{-1}(J\omega)^{-n} \tag{13}$$

where *Q*and *n* are associated with CPE and exponent respectively, $j^2 = -1$ is regarded as imaginary axis, ωstand for angular frequency in$rads^{-1}$,($\omega = 2\pi f$explain frequency in H_Z), $R_S$signifies solution resistance, *W*denotes the Warburg parameter and *n* is the considered shifting factor, it is in assortment of −1 to 1. If $n = -1$(an inductor), $n = 0$(real resistor) and $n = 1$(capacitor) [47–49]. Double layer (C_{dl}) and film capacitance (*Cf*) are evaluated and defined byY_0,*n*, ω as shown in Eq. (14) [49].

$$C = Y_0(\omega)^{n-1} = Y_0(2\pi f_{Zim-Max})^{n-1} \tag{14}$$

The goodness of EIS data fit to model is χ^2 factor, described as [50]

$$\chi^2 = \sum_{i=1}^{n}\left[\frac{\left(Z_i'\left(\omega_i,\vec{P}\right)-a_i\right)^2}{a_i^2+b_i^2} + \frac{\left(Z_i''\left(\omega_i,\vec{P}\right)-b_i\right)^2}{a_i^2+b_1^2}\right] \tag{15}$$

where $\omega_i, a_i, b_i$are the experimental data points, $\vec{P}$is a factor connected with the proposed model andZ_i'andZ_i'' are expected data points (calculated). As listed in Table 3 the χ^2 values are slightly small ($\angle 1\times10^{-3}$), showing excellent fitness of available EIS plot (Fig. 3d) to proposed circuit model [51]. Close scrutiny of Fig. 3a revealed that the addition of inhibitor results in an increase in the diameter of the semi-circle in the Nyquist plot. An increase in the diameter of the semi-circle in the Nqyuist plot is attributed strengthening of the adsorbed film formed by the active molecules of dexamethasone drug. The formation of the protective film layer on the steel surface is believed to be the culprit of the observed suppression in the cathodic

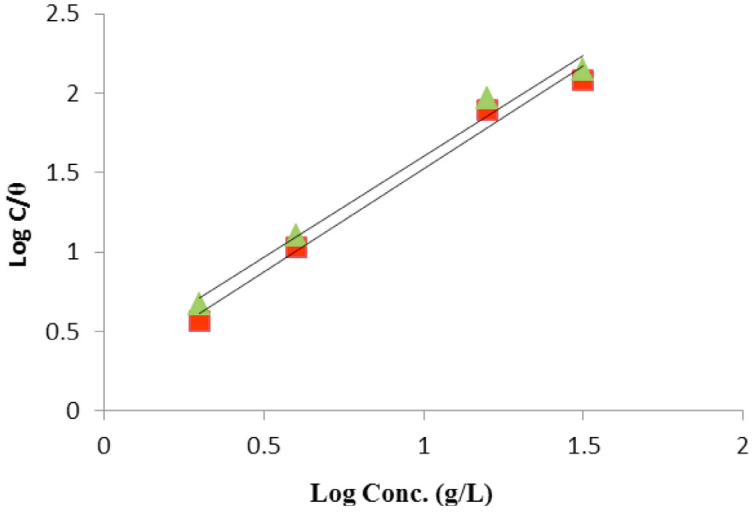

Fig. 2. Langmuir isotherm plot of Log(C/θ) versus Log C for M-steel in 2 M HCl containing DM at different temperatures.

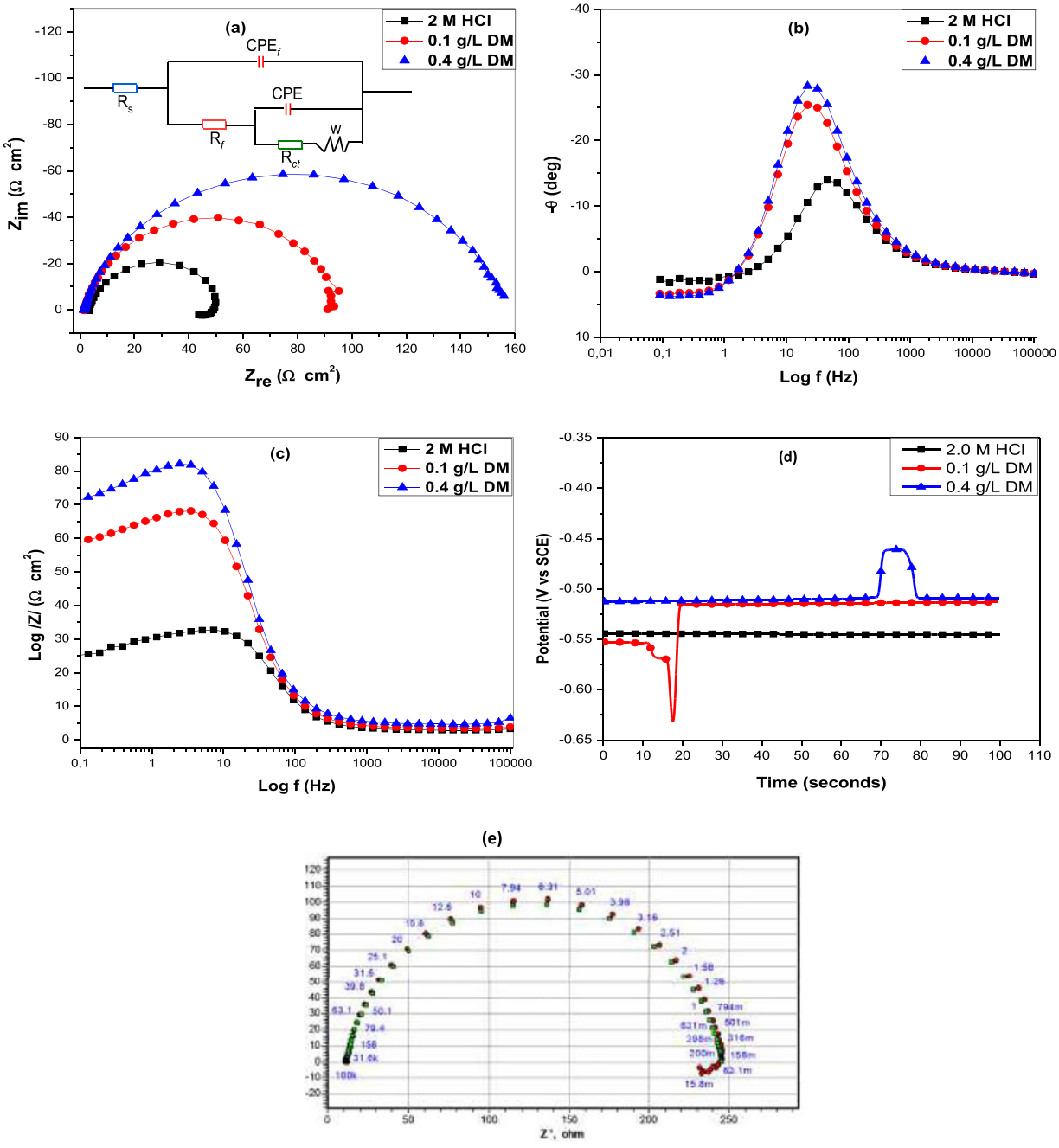

Fig. 3. Electrochemical impedance plot of MS in 2 M HCl solution in the absence and presence DM of (a) Nyquist (b) Bode phase angle plot and (c) Bode modulus plot (d) OCP plot (e) fitting curve.

and anodic partial reactions [52]. The increase in the diameters and in the low frequency impedance magnitude (/Z/0.05 Hz) was found to depend on concentration of Dexamethasone compound. In high frequency region the presence of DM in the phase angle maximal became higher than that of the uninhibited solution which results to the formation of protective film and increase in surface coverage on the steel surface [53]. The OCP versus time plot for mild steel in the blank solution and with different concentrations of the Dexamethasone drug is shown in Fig. 3d. From the plot, the OCP of 2 M HCl acid solution was found to be −0.55 V. For an increase in concentration of inhibitor from 0.1 g/L to 0.4 g/L, the OCP shifted towards the noble direction from −0.51 to −0.52 V, indicating that Dexamethasone controls mainly anodic metal dissolution reaction. Further observation revealed that the blank solution stabilizes from the point of

Table 3
Electrochemical parameters of mild steel in 2 M HCl in absence and presence of DM.

System	R_S(Ωcm²)	R_{ct}(Ωcm²)	n	C_f(μFcm⁻²)	C_{dl}(Fcm²)	*IE*(%)	χ^2(x 10⁻⁴)
2 M HCl	1.659	50.8	0.86	21.02	2.343E−5	–	8.16
0.1 g/L DM	2.820	94.1	0.88	10.53	3.919E−5	60	9.50
0.4 g/L DM	3.306	157.8	0.89	9.19	3.216E−5	81.8	9.30

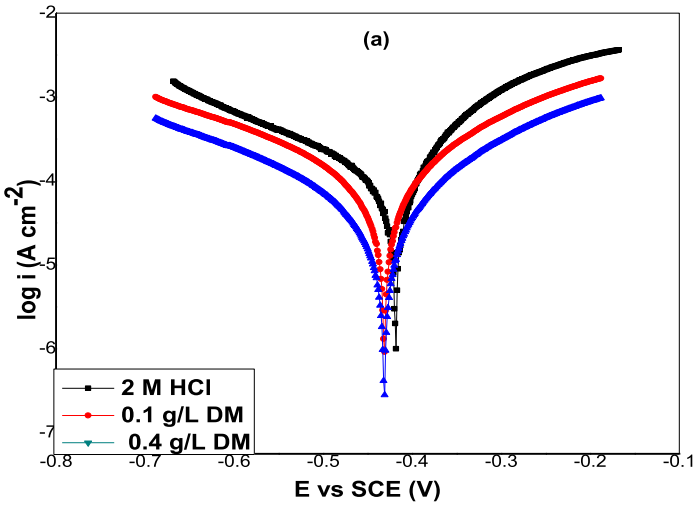

Fig. 4. Potentiodynamic polarization curves of mild steel in 2 M HCl solutions in the absence and presence of Dexamethasone (DM).

immersion. Also the inhibited medium 0.1 g/L^{-1} reaches a steady state condition after 19 s while that of 0.4 g/L^{-1} stabilizes after 80 s, suggesting that the potential evolves towards the stable values during the period of study. Table 3 shows the results obtained from the EIS, noticeably the $R_{ct}(\Omega cm^2)$ values and the efficiency of the inhibitor

Table 4
Polarization data for mild steel in 2 M HCl in the absence and presence of DM.

System	E_{Corr} (mV vs. SCE)	I_{Corr} (μA cm^{-2})	b_C (mV dec^{-1})	b_a (mV dec^{-1})	*sc* (θ)	*IE*(%)
2 M HCl	−466.3	312.7	120.1	95.0	–	–
0.1 g/L DM	−459.3	85.4	108.7	78.1	0.72	72
0.4 g/L DM	−463.8	53.6	101.2	73.2	0.83	83

(IE%) is seen to increase on addition of the drug compound. One unique observation is that as the consistence of DM increases, C_{dl} and$C_f$exhibited opposite trend, which reveal on the MS surface adsorb DM molecule and charge transfer phenomenon. Also the numerical values of the shifting factor "*n*" evaluates the non-ideal capacitive trend due to unevenness of the electrode and surface micro-defects. The constant phase element represented by double layer capacitance values confirmed the presence of the Dexamethasone compound on the surface of the steel leading to the decrease in the dielectric constant and increasing the thickness of the double layer. This is because organic species shown minimum dielectric influence than inorganic species [54].

3.4. Potentiodynamic polarization

Polarization plot for mild steel in the blank and inhibited solution (0.1 g/L^{-1}- 0.4 g/L^{-1}) of DM at 30°C is shown in Fig. 4. The nature of

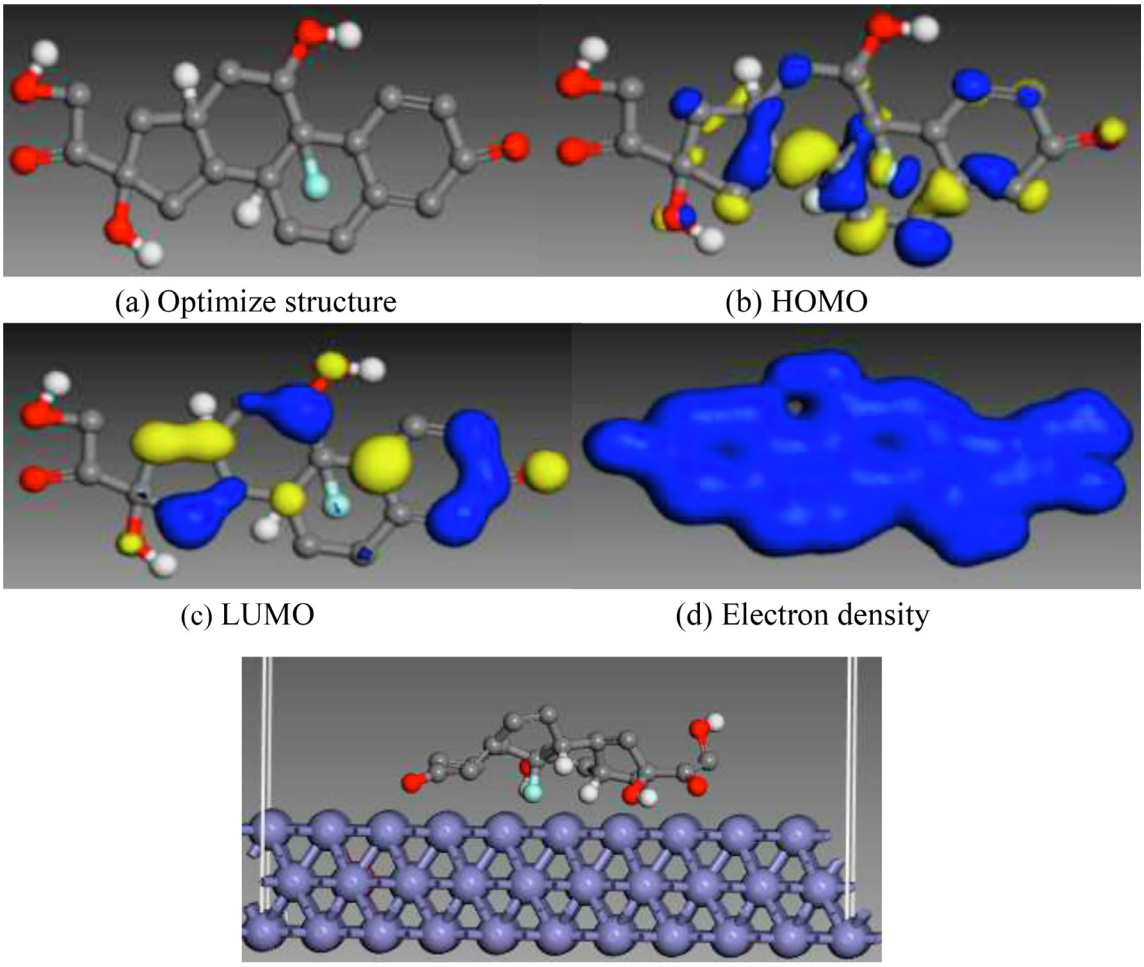

Fig. 5. Electronic structures of neutral form of Dexamethasone (a) Optimized structure (b) HOMO (c) LUMO (d) Electron density and (e) Snapshot of DM molecule.

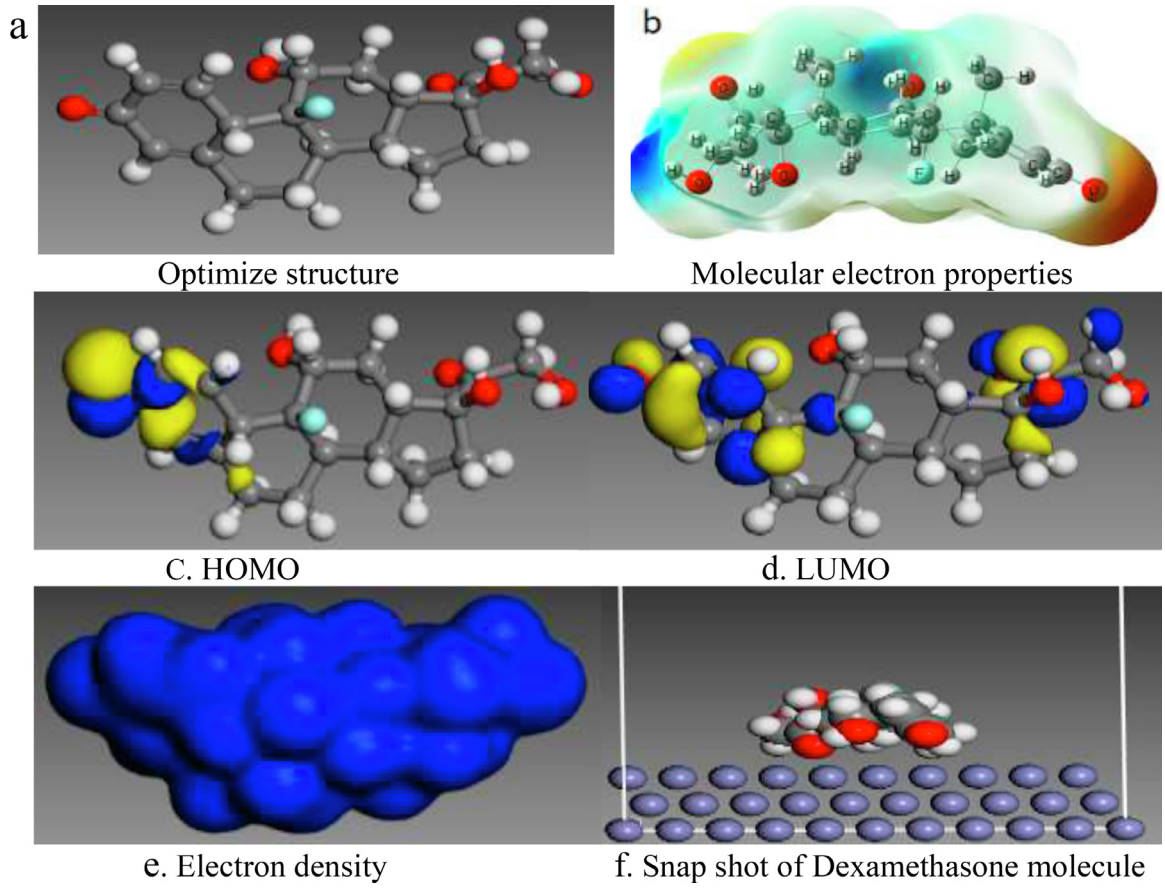

Fig. 6. Electronic structures of protonated form of Dexamethasone (a) Optimized structure (b) MEP (c) HOMO (d) LUMO (e) Electron density and (f) Snapshot of DM molecule.

the plot in the blank and at varying DM concentrations is comparable [55]. Increase in DM concentration obstructs the anodic and cathodic reactions. Vital parameters considered in this investigation includes; corrosion potential (E_{corr}), tafel slopes (b_a&b_c) and corrosion current density (I_{corr}) as well as (*IE%*) are presented in Table 4. The (E_{corr})values were marginally modified by adding 0.1 g/L^{-1}- 0.4 g/L^{-1}DM in 2 M HCl, which shows that the impact of DM is significant. However, literature findings suggested that for an inhibitor to be categorized as a cathodic or anodic mode, a precise range or acceptable deviation in corrosion potential(E_{corr}) should be ± 85 mV/SCE [56]. From our investigation, the(E_{corr}) values were less than 85 mV, postulating that DM was a mixed type inhibitor [57–58]. The description of our findings denotes that the active molecules of DM adsorbed by impeding the active sites of mild steel surface, resulting in a significant reduction in the area needed for corrosion. As listed in Table 4, the numerical values for(b_a&b_c)decline bit by bit with rise in DM concentration. The trend of $b_a$and$b_c$scrutinizes the symmetry of the activation energy for both side reactions [59]. Thus the DM thin film had a positive influence on anodic and cathodic axis with predominant anodic effect. (I_{corr}) value also decline slightly from 0.1 g/L^{-1}–0.4 g/L^{-1} DM, signifying that (IE%) is promoted with increase in DM concentration.

3.5. MD-simulation concept

MD-simulation was used to explain the details of mechanism of the corrosion inhibition process of the study molecule [60]. For the neutral form, the optimize structure, HOMO, LUMO, electron density and the snap shot are shown in Fig. 5 while the protonated form are shown in Fig. 6. Donor-acceptor relationship is due to the adsorption of organic molecules on the metallic surface. The ability of the molecule to donate electron or accept electron is represented by HOMO and LUMO. The vital parameters of the quantum chemical study include energy of highest occupied molecular orbital E_{HOMO}, energy of lowest unoccupied molecular orbital E_{LUMO}, energy gab ΔE, electronegativity χ, global hardness η, global softness σ and the number of electron transfer ΔN are shown in Table 5. The high electron donating and accepting abilities of the Dexamethasone are associated with high values of E_{HOMO} and low value of E_{LUMO} respectively which shows bonding between the inhibitor molecule and the surface of the steel [61]. The energy gab parameter describes the relationship between metal-inhibitor interactions. The smaller the value of energy gab ΔE is associated with a global softness of the studied molecule which indicated a good inhibition efficiency of the molecule, while

Table 5
Calculated quantum chemical parameters of the Dexamethasone molecule.

E_{HOMO}	E_{LUMO}	ΔE (eV)	*IP*(eV)	EA (eV)	χ(eV)	η(eV)	σ	*Eads*	ΔN/e
Neutral form									
−6.284	−6.280	4×10^{-3}	6.284	6.280	6.282	2×10^{-3}	500	137.3	7.2×10^{-3}
Protonated form									
−5.045	−2.347	2.698	5.045	2.347	3.696	1.349	0.741	168.7	0.4166

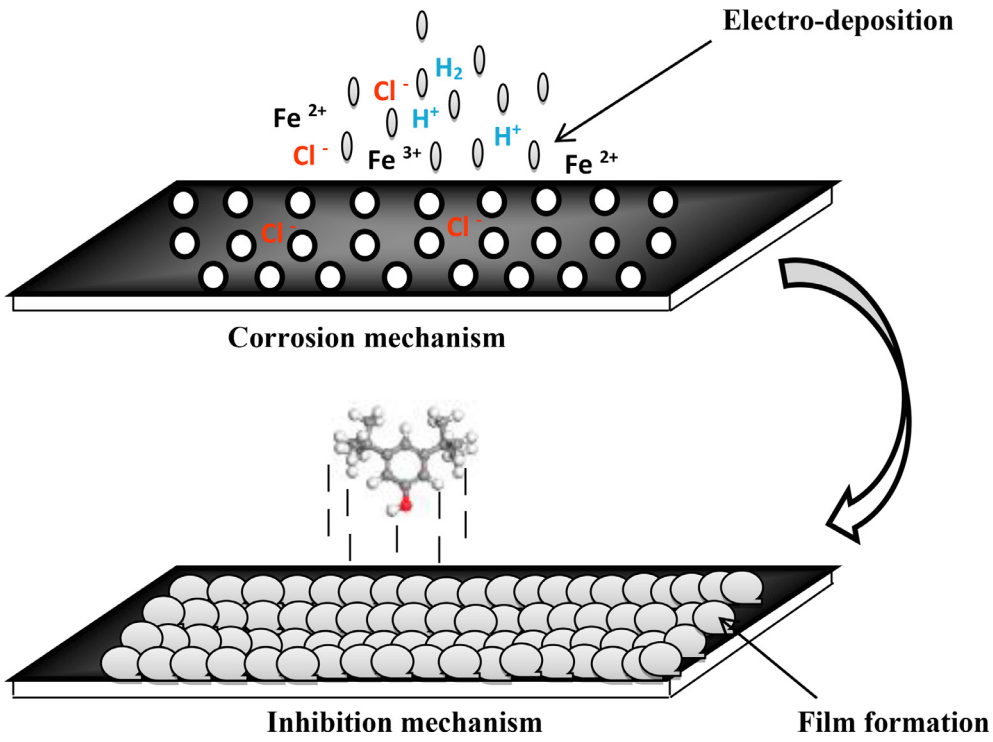

Fig. 7. Schematic representation of the adsorption of DM molecule against MS corrosion.

the higher value of energy gab ΔE is associated with global hardness, reflecting that the inhibitor is not capable of performing well as a corrosion inhibitor. The important parameters required for the calculation of electronegativity χ, global hardness η, global softness σ are the ionization potential (IP) and electron affinity (EA) obtained from the E_{HOMO} and E_{LUMO} according to equations below [62].

$$\chi = \frac{IE + EA}{2} \tag{16}$$

$$\eta = \frac{IE - EA}{2} \tag{17}$$

$$\sigma = \frac{1}{\eta} = -\frac{2}{E_{HOMO} - E_{LUMO}} \tag{18}$$

The values of electronegativity χ and global hardness η were used in estimating the number of electrons transfer ΔN based on Eq. (19) [63].

$$\Delta N_{110} = \frac{\Phi - \chi_{inh}}{2(\eta_{Fe} + \eta_{inh})} \tag{19}$$

The derive work function (φ), theoretical value given as φ= 4.82 according to [64]. The number of electrons transfer always take place from the inhibitor molecule to the metal surface. When the value of electron transfer ΔN is greater than zero it signifies a greater electron donating ability of the inhibitor to the metal surface, also when the value of the electron transfer ΔN is less than 3.6 it reflect the effectiveness of the Dexamethasone molecule. In our present study the value of ΔN is positive showing better performance in the neutral form. The estimated value for the energy gap also supported inhibitory performance of the DM molecule. Also the chemistry of Dexamethasone is very vital, DM is a fluorinated steroid that is replaced by hydroxyl groups at positions 11, 17 and 21, a methyl group at position 16 and oxo groups at positions 3 and 20. It is a member of the type of glucocorticoids. DM has electro-active oxygen and carbon atoms with aromatic ring (rich electrons). From the quantum chemical point of view, Figs. 5a and 6a show the optimized structure of DM and Fig. 6b illustrates the molecular electrostatic potential (MEP) plot for the DM molecule. As shown, the colors for the MEP surface are according to red for (−ve) charge; blue for (+ve) charge; light blue represents slightly electron rich areas; green for neutral respectively. In case of our results, the partial negative charges are mainly localized over the carbonyl group (red color), the site where HOMO is located which can interact with the mild steel, while the LUMO level is seen at the carbon atom having the tendency of accepting electrons. Total electron density plot for the most stable configuration is displayed in Fig. 6e. As can be easily seen from Fig. 6e, a significant charge transfer has occurred due to the interaction of the DM molecule with the mild steel. Also the carbonyl groups conjugated with a double bond undergo adsorption in comparison with the isolated carbonyl group. The adsorption of unconjugated carbonyl group is activated by the neighboring hydroxyl groups. The carbonyl group at position 20 is activated by the hydroxyl groups present at position 17 and 21.

Table 6
8 Membership functions selected for ANFIS modeling.

Membership functions	Error value
trimf	2.1685
trapmf	1.6195
gbellmf	1.4547
guassmf	1.5466
guass2mf	1.6194
pimf	1.6342
dsigmf	1.6264
psigmf	1.6274

3.6. Mechanism of corrosion inhibition

From the experimental results obtained from different techniques. It can be inferred that dexamethasone drug inhibits the corrosion of mild steel in 2 M HCl by adsorption of active molecules at metal /solution interface. It is generally known that the adsorption of inhibitors at the metal surface is the first stage in the mechanism of the

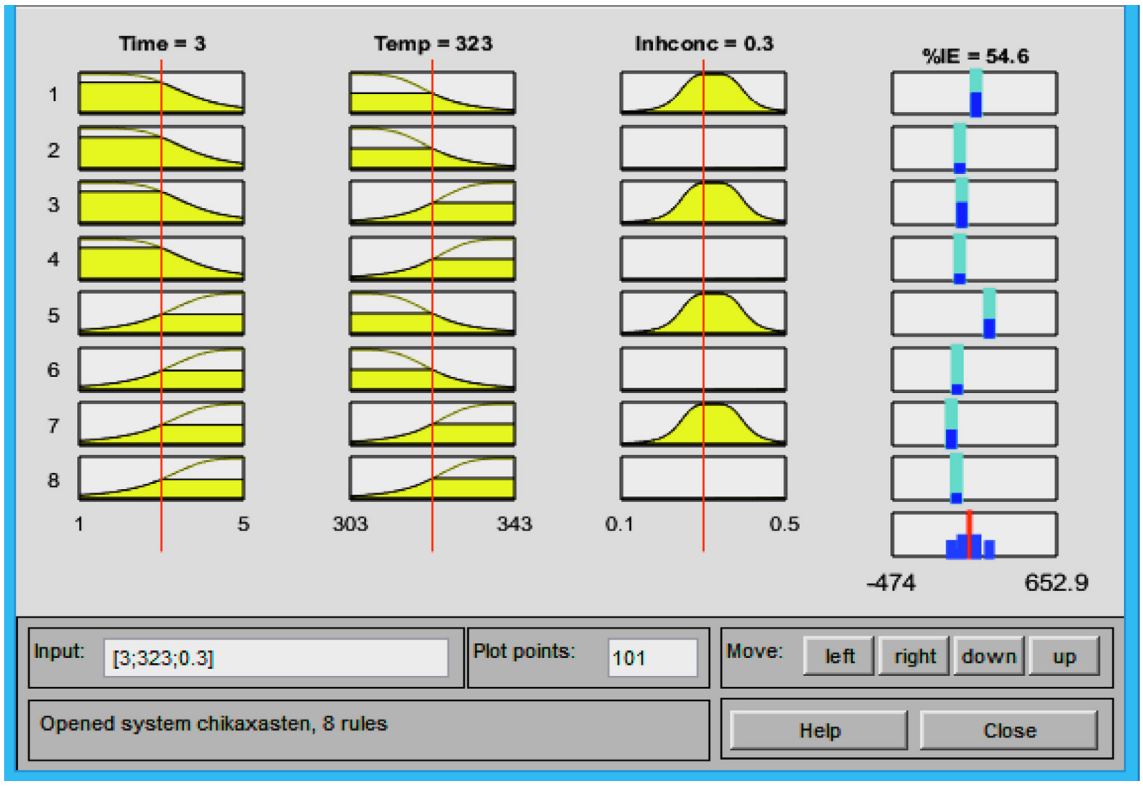

Fig. 8. ANFIS rules for input and output response.

inhibitor action. Active molecules of an inhibitor may be adsorbed on the metal surface in different ways; (i) electrostatic /mutual interaction between the protonated form of the inhibitor and adsorbed counter chloride ion (physisorption),(ii) donor–acceptor relationship between electron pairs of heteroatoms and vacant d-orbital of Fe surface atoms (chemisorption), (iii) donor–acceptor relationship between the π – electrons of aromatics rings and multiple bonds and vacant d-orbitals of Fe surface atoms (chemisorption) and a combination of types (I and III). The inhibition of active dissolution sites of the metal is attributed to the adsorption of dexamethasone active molecules on the MS surface forming a dense film layer. The active molecules can be adsorbed onto the MS surface through electron transfer from adsorbed species to the vacant electron orbital of low/minimum energy in the metal to form a co-ordinate type of bond. Inhibitory action of an inhibitor depends on many factors [35] including number of feasible adsorption areas, mode of interaction with metal surface, molecular size and the heterocyclic structure. The schematic illustration of adsorption orientation of Dexamethasone drug on MS surface is shown in Fig. 7. The active molecules can share their lone pair with empty orbitals of metal cations, so the steel surface can be shield by a protective film layer. This results in the formation of a barrier film with capability of ions, oxygen and water diffusion restrictions on the steel surface.

Table 7
Experimental and ANFIS prediction.

No of runs	Expected	ANFIS Pred.
1	30	30.9197
2	50	47.6779
3	61.54	63.7874
4	80.17	80.4107
5	69.05	69.4095
6	24.39	24.6766
7	46.34	44.603
8	56.1	58.7618
9	80.17	80.4107
10	70.73	70.759
11	22.22	21.8933
12	47.06	47.9118
13	80.17	80.4095
14	69.05	69.4095

3.7. *Adaptive-Neuro fuzzy inference system prediction*

ANFIS program in MATLAB was used to design a model to predict the efficiency of DM drug as a potential inhibitor. In ANFIS environment, the experimental data was split into 3 sections for training, testing and validation. Gaussian membership was used for input and linear membership used for output. Training section comprises of 80% data while 20% was attributed to testing section [65]. Number of iterations required to achieve minimum steady state error was 30 epochs and two triangular membership functions attached to each of the independent variables. With a total of 3 independent variables, the total number of constant membership functions used for the dependent variable was eight membership functions as seen in Table 6 which resulted in generation of eight inference rules (the yellow color region denote the membership function of the input data while blue region is the second phase of the fuzzy rule as presented in Fig. 8). The ANFIS response was obtained and de-normalized to obtain accurate ANFIS prediction. ANFIS prediction based on the R^2 is presented in Table 7 considering 14 runs. From the ANFIS architecture (Fig. 9) the input neuron is 3 (each neuron denotes the independent variables) with the input neuron attached to 2 neurons indicating 2 membership functions used for each independent variable. The hidden neurons correspond with the output neurons where each of the neurons in the hidden layer is connected to the neurons in the output layer. The single neuron at the extreme right indicates the dependent variable which is one. The model

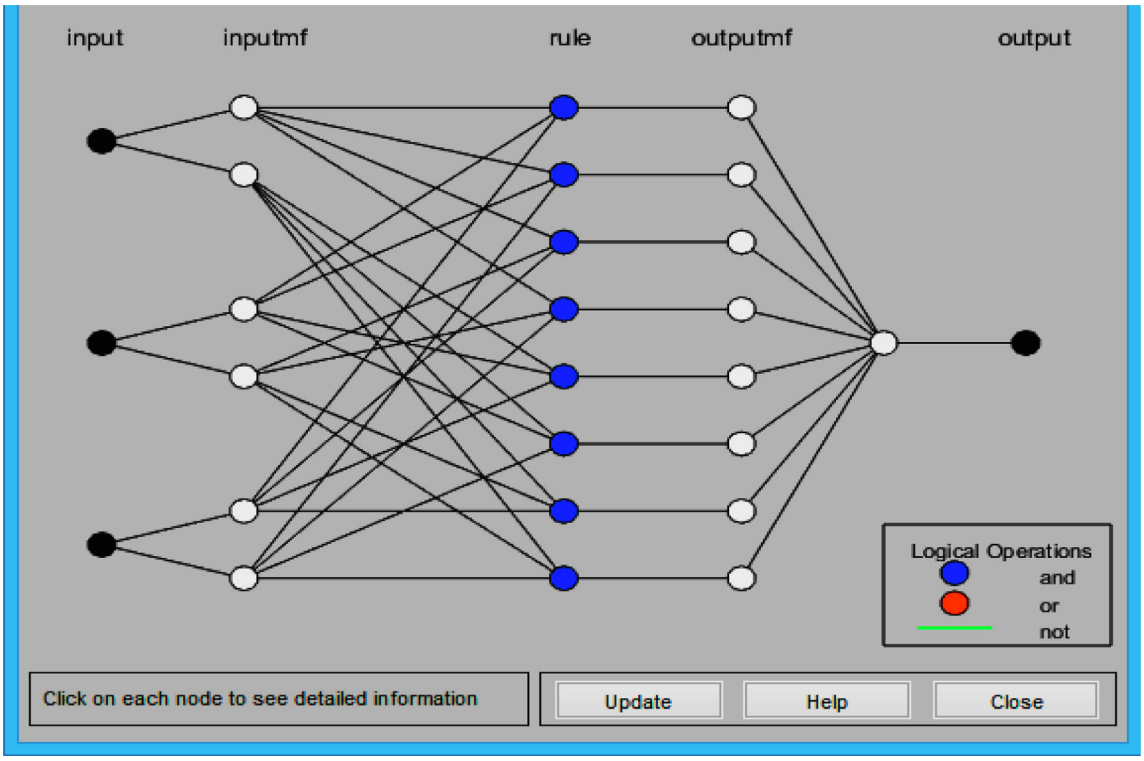

Fig. 9. Architectural design of ANFIS model.

systematically gave accurate prediction with optimum value of 80%. The accuracy/conformity of the predicted values is clearly affirmed by the statistical factor R^2 0.993 which denotes excellent model status as shown in Fig. 10a. Since the proposed ANFIS model obeyed the criteria of having its R^2-value greater than 90%, it made it the most preferred model to carry out further test [66]. As such, surface

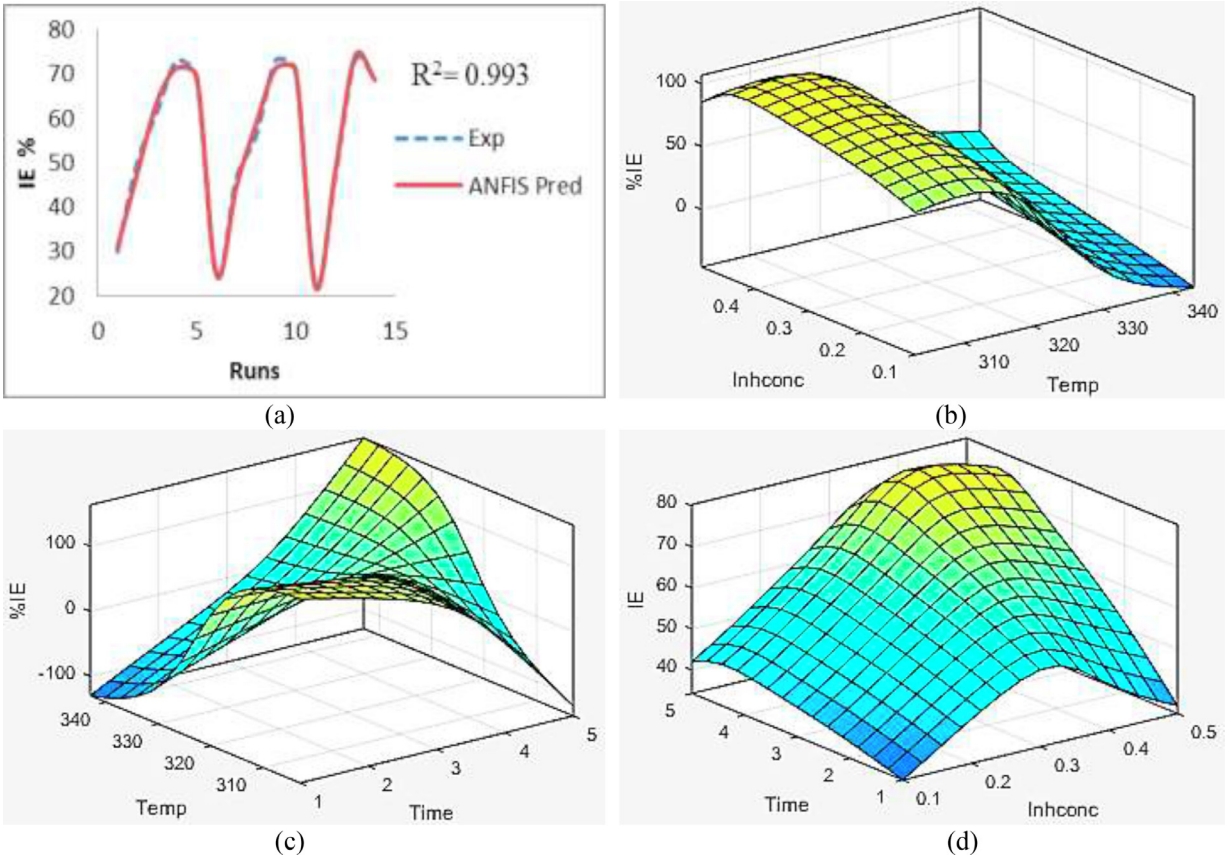

Fig. 10. (a) Exp. vs. ANFIS Pred. (b) Surface viewer plots for independent variables with expected response.

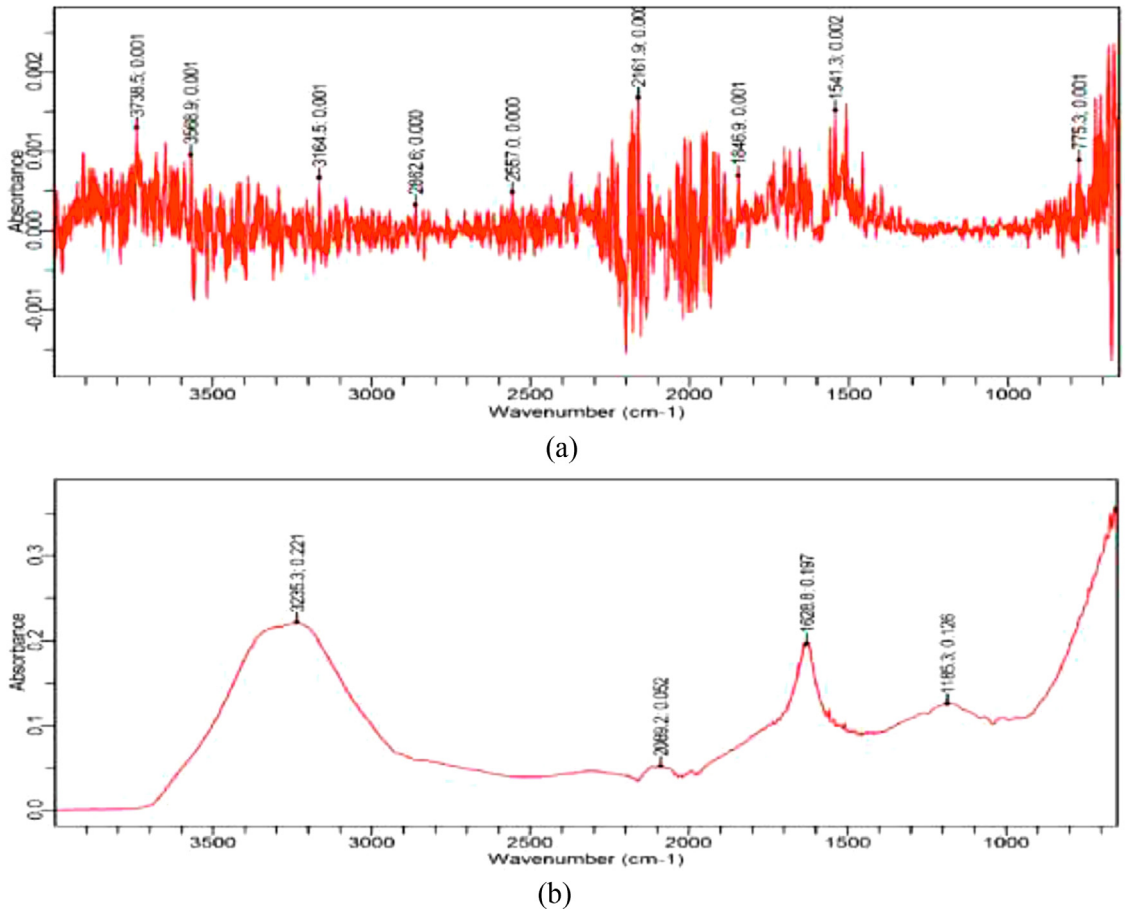

Fig. 11. FTIR spectra for (a)Dexamethasone drug and (b) adsorbed molecules on MS surface.

viewer plots of ANFIS prediction with respect to the interaction parameters were also considered vital. The surface viewer plots pin points the effect of interaction parameters (coding the independent variables as *x* and *y* axis of the 3D plots) against inhibition efficiency. It is pertinent to graphically obtain the independent parameters that gave the optimal value via ANFIS prediction. Thorough inspection of Fig. 10b explain that systematic increase in DM concentration increases the inhibition efficiency (IE%), on the contrary a slight diminution curve was evidently seen at elevated temperatures, The decline in (IE%) from 333 to 343 K temperatures demonstrated Dexamethasone's instability when it is exposed to higher temperatures, which also prove that the DM active molecule was disperse at elevated corrosive conditions. Fig. 10c gives additional insight on the nature of interaction between temperature and time. At early immersion period of adsorption phenomenon, the positively charge DM molecules initiates spontaneous competition with H^+ for electrons on the MS thereby impeding the chloride ions that necessitates corrosion [35]. This led to a near perfect or uniform surface coverage by DM molecules. The efficiency declined slightly after 4 h of immersion. Further insight shows that the corrosion rate (CR) increased rapidly with prolonged immersion period at 343 K due to dispersion of DM active molecules. The interactive effect between time and inhibitor is highlighted in Fig. 10d. The DM efficiency rises and consequently attains equilibrium point of 80% at 4 h of study at optimum range of DM. Furthermore, it slightly decline afterwards. This implies that the Max $_{IE\%}$ is attainable within 4 h of immersion. However, taking into consideration of both independent factors, efficiency of DM drug is attainable and stable at optimum range and medium immersion time.

3.8. Surface characterization analysis

Earlier researchers have reported that the FTIR spectrometer is a strong instrument which can be used to prove the form of organic inhibitors bonding adsorbed on the metal surface [67]. The protective film formed on a metal surface was analyzed using FTIR spectra. FTIR of pure Dexamethasone is given in Fig. 11a. It evidenced the existence of O—H, N—H, C—O, C=O groups. The FTIR spectra of the film layer formed on the metal surface after immersion for 5 h in 2 M HCl containing 0.4 g/L of Dexamethasone is shown in Fig. 11b. Nearly all the peaks observed for the pure compounds were also present in the adsorbed specie (corrosion products), with some slightly changes or modification after molecular adsorption. Further observation reveals that after adsorption of the molecules most of the peaks appeared weaker. The FTIR bands of the compounds with slight changes and the absence of few bands suggest an interaction between the compounds and the metal surface resulting in the formation of a protective film layer [27, 68].

3.8.1. SEM, EDX and AFM studies

So as to understand the level of protection of MS surface by DM more clearly, micrographs of the steel in blank and inhibited system were closely scrutinized using SEM technique. In the blank solution (Fig. 12a) a coarse, dark pits and uneven surface fractions were observed with various macro pores. The corrosion topography is visible enough due to hostile nature of chloride ions in the facial dissolution layer of the steel [69]. Inversely, the micrograph of the steel from inhibited medium (Fig. 12c) evidently differs from the control sample (appears smooth). The level of iron oxide form is suppressed due to

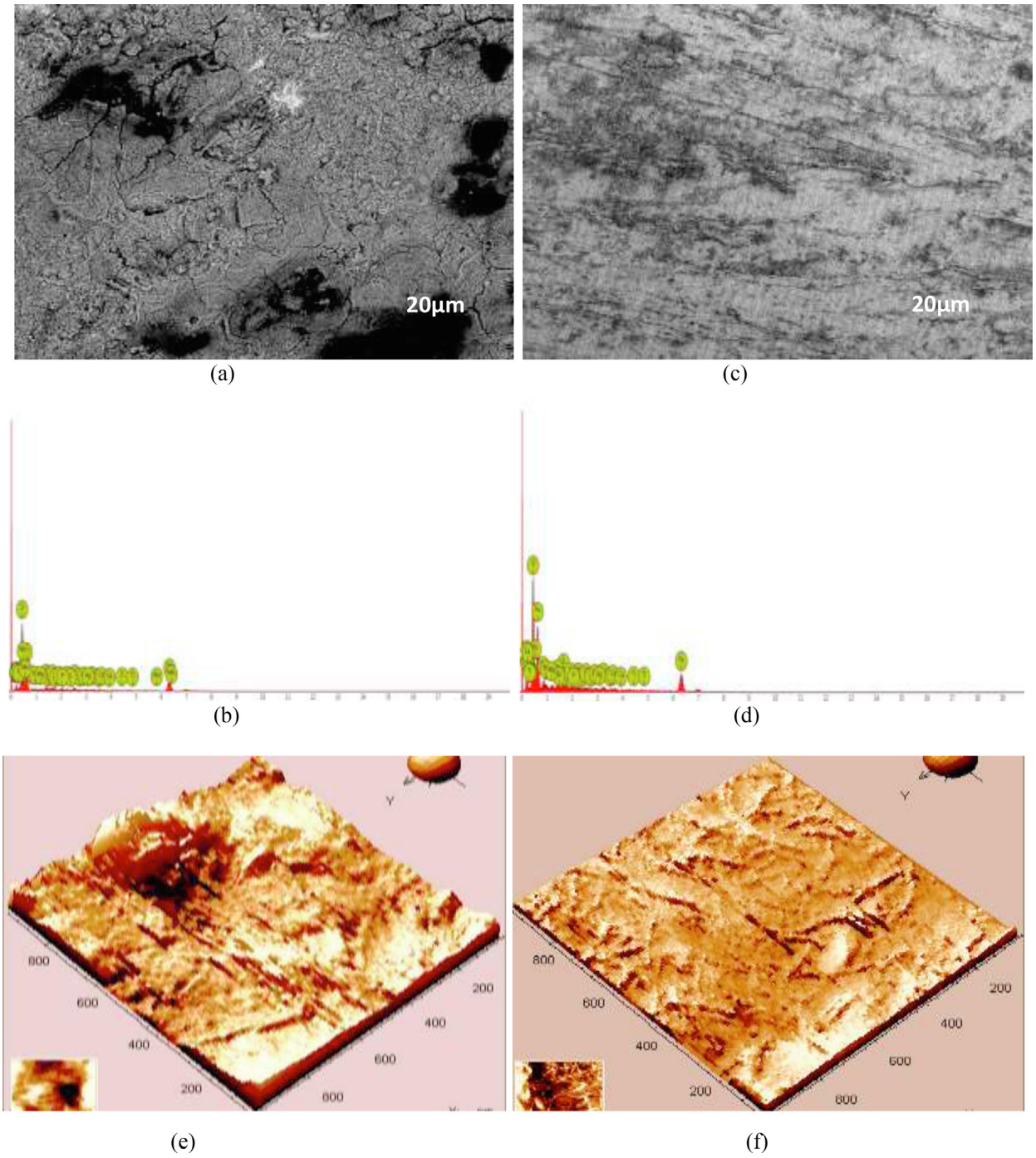

Fig. 12. SEM Micrographs, EDX and AFM images of mild steel in (a-b) 2 M HCl (c-d) 2 M HCl + 0.4 g/L DM (e) AFM / MS in 2 M HCl (f) AFM /MS in 2 M HCl + 0.4 g/L DM.

the physical formation of a dense film on the facial layer of the steel [70]. The great deal of activeness of DM is enormously dependent on dosage of the studied inhibitor. Also EDX is a vital analytical instrument for evaluation of elemental composition on the steel surface prior to and after DM immersion. In Fig. 12b the densely particles deposited on the steel enormously comprises of iron oxides in devoid system. On the contrary, in the inhibited area Fig. 12d several peaks like O, Ca, Si and Fe were added and an increase in Fe peaks evidently describe that DM molecules obstruct the invading of electrolyte species [71]. Atomic force microscope (AFM) is an effective method for examining surface morphology, and it is also useful in corrosion inhibition studies to evaluate the nature of film formation on metal surface. Fig. 12e and 12f indicates the AFM images of polished mild steel in 2 M HCl with and without the presence of 0.4 g/L^{-1} Dexamethasone molecule. In HCl, the AFM picture of the mild steel surface appears more degraded than in HCl with 0.4 g/L^{-1}Dexamethasone drug. In addition, the typical average roughness of polished mild steel in a blank solution of 2 M HCl was calculated to be 238 nm, peak to valley was recorded as 78.4 nm and the average roughness was reduced to 98 nm, peak to valley was 43.7 nm when the inhibitor (DM) was added to the blank solution which indicated the formation of a film layer on the mild steel surface [72–73].

4. Concluding remarks

From the available data set obtained, the following points can be inferred.

DM is a strong corrosion inhibitor in 2 M HCl solution for protection of mild steel by intercepting both anodic and cathodic reactions (Mixed type inhibitor).

The inhibitory action of DM drug depends on its concentration. For appropriate safety this inhibitor should be applied at high concentrations.

Langmuir adsorption isotherm best reflects that the process of inhibition of corrosion occurs only by physical adsorption.

MD-simulation concept provides detailed information on feasible adsorption areas of DM drug.

Measurements of surface analysis are in good agreement with the experimental findings and indicate a safe and well distributed film over the metal surface. In the 2 M HCl solution containing inhibitor, a substantial diminution in surface roughness was seen as opposed to the solution without DM.

ANFIS model best predicted the non-linear interactions between the multi input and single output response with optimum value of 80% and R^2 0.993.

Declaration of Competing Interest

The authors declare that they have no conflict of interest.

Funding

No funding was received for this research

References

[1] Ihebrodike MM, Nwandu MC, Okeoma KB, Nnanna LA, Chidiebere MA, Eze FC, Oguzie EE. Experimental and theoretical assessment of the inhibiting action of *aspilia africana* extract on corrosion aluminum alloy AA3003 in hydrochloric acid. J Mater Sci 2012;47:2559–72.
[2] Sedik A, Lerari D, Salci A, Athmani S, Bachari K, Gecibesler IH, Solmaz R. Dardagan fruit extract as eco-friendly corrosion inhibitor for mild steel in 1M HCl: electrochemical and surface morphological studies. J Taiwan Inst Chem Eng 2020;107:189–200.
[3] Dehghani A, Bahlakeh G, Ramezanzadeh B, Ramezanzadeh M. Electronics/ atomic level fundamental theoretical evaluations combined with electrochemical/surface examinations of Tamarindus indiaca aqueous extract as a new green inhibitor for mild steel in acidic solutions (HCl 1M). J Taiwan Inst Chem Eng 2019;102:349–77.
[4] Asadi N, Ramezanzadeh M, Bahlakeh G, Ramezanzadeh B. Utilizing lemon balm extract as an efficient green corrosion inhibitor for mild steel in 1M HCl solution: a detailed experimental, molecular dynamics, Monte Carlo and quantum mechanics study. J Taiwan Inst Chem Eng 2019;95:252–72.
[5] Dehghani A, Bahlakeh G, Ramezanzadeh B, Ramezanzadeh M. Detailed macro-/micro scale exploration of the excellent active corrosion inhibition of a novel environmentally friendly green inhibitor for carbon steel in acidic environment. J Taiwan Inst Chem Eng 2019;100:239–61.
[6] Elmsellem H, Ouadi Yassir El, Majda M, Hajar B, Hanae S, Abdelouahed A, Ahmed MA, Ibrahim AR, Heri SK, Belkheir H. A natural antioxidant and an environmentally friendly inhibitor of mild steel corrosion: a commercial oil of basil (Ocimum Basilicum L.). J Chem Technol Metall 2019;4:742–9.
[7] Hegazi MA, Nazeer AA, Shalabi K. Electrochemical studies on the inhibition behavior of copper corrosion in pickling acid using quaternary ammonium salts. J Mol Liq 2015;209:419–27.
[8] Zakiyeh M, Mansour R. The use of green *bistorta officinalis* extract for effective inhibition of corrosion and scale formation problems in cooling water system. J Alloys Compd 2017;770:669–78.
[9] Akhil S, Kamal KT, Nishant B. Electrochemical studies and surface examination of low carbon steel by applying the extract of *Musa acuminate*. Surf Interfaces 2020;18:100436.
[10] Fekkar G, Yousfi F, Elmsellem H, Aiboudi M, Ramdani M, Abdel-Rahman I, Hammouti B, Bouyazza L. Eco-friendly Chamaerops humilis L. fruit extract corrosion inhibitor for mild steel in 1M HCl. Int J Corros Scale Inhibit 2020;9(2):446–59.
[11] Wilfred E, Run-Hua Z, Okafor PC, Xing-Wen Z, He Tao, Wei Kun, Xiu-Zhou L, Chun-Ru C. Adsorption and corrosion inhibition performance of multi-phytoconstituents from *Dioscorea septemloba* on carbon steel in acidic media: characterization, experimental and theoretical studies. Colloids Surf A 2020;590:124534.
[12] Shabani-Nooshabadi M, Hoseiny FS, Jafari Y. Green approach to corrosion inhibition of copper by the extract of *calligonum comosum* in strong acidic medium. Metall Mater Trans A 2015;46:293–9.
[13] Gece G. Drugs: a review of promising novel corrosion inhibitors. Corros Sci 2011;53:3873–98.
[14] Abeng FE, Anadebe VC, Idim VD, Edim MM. Anti-corrosion behavior of expired tobramycin drug on carbon steel in acidic medium. S Afr J Chem 2020;73:125–30.
[15] Ikpi ME, Abeng FE. Electrochemical and quantum chemical investigation on adsorption of Nifedipine drug as corrosion inhibitor at API X-52 steel /HCl acid interface. Arch Metall Mater 2020;65:125–31.
[16] El-Haddad MN, Fouda AS, Hassan AF. Data from chemical, electrochemical and quantum chemical studies for interaction between Cephapirin drug as an eco-friendly corrosion inhibitor and carbon steel surface in acidic medium. Chem Data Collect 2019;22:100251.
[17] Geethamani P, Kasthuri PK. The inhibitory action of expired asthalin drug on the corrosion of mild steel in acidic media: a comparative study. J Taiwan Inst Chem Eng 2016;63:490–9.
[18] Sumayah B, Abhinay T, Hassane L, Chungb Ill-Min, Ashish K. Corrosion inhibition efficiency of bronopol on aluminium in 0.5M HCl solution: insights from experimental and quantum chemical studies. Surf Interfaces 2020;20:100542.
[19] Abdallah M, Gad EAM, Sobhi M, Al-Fahemi JH, Alfakeer MM. Performance of tramadol drug as a safe inhibitor for aluminum corrosion in 1.0M HCl solution and understanding mechanism of inhibition using DFT. Egypt J Pet 2019;28:1713. -181.
[20] Iman D, Ramesh Kumar S, Rashvander Avei M, Vijayan M. Electrochemical and quantum chemical studies on corrosion inhibition performance of 2,2'-(2-Hydroxyethylimino)bis[N-(alphaalpha-dimethylphenethyl)-N-methylacetamide] on mild steel corrosion in 1M HCl solution. Mater Res 2020;23(2):e20180610.
[21] Amina B, Hana F, Souad D, Rachid S, Hana L, Yasser BA, Alessandro E, Marco B, Yacine B. Computational and experimental studies on the efficiency of *Rosmarinus officinalis* polyphenols as green corrosion inhibitors for XC48 steel in acidic medium. Colloids Surf : Physiochem Eng Aspects 2020;606:125458.
[22] Chinedu MA, Matthew MC, Ekwe BE, Albert CA. Modeling & optimization of terminalia catappa L. kernel oil extraction using response surface methodology and artificial neural network. Artif Intell Agric 2020;4:1–11.
[23] Onu CE, Igbokwe PK, Nwabanne JT, Nwajinka CO, Ohale PE. Evaluation of optimization techniques in predicting optimum moisture content reduction in drying potato slices. Artif Intell Agricult 2020;4:39–47.
[24] Ofoefule AU, Esonye C, Onukwuli OD, Nweze E, Ume CS. Modeling and optimization of african pear seed oil esterification and transesterification using artificial neural network and response surface methodology comparative analysis. Ind Crops Prod 2019;140:111707.
[25] Dhaybia D, Elmsellem H, El-Hassane A, Lei G, Baraa H, Burak T, El-Louzia Ahmed, Khalid B, Khalid K, Banacer H. Anti-corrosion performance of 8-hydroxyquinoline derivatives for mildsteel in acidic medium: gravimetric, electrochemical, DFT and molecular dynamics simulation investigations. J Mol Liq 2020;308:113042.
[26] Nnaji PC, Anadebe VC, Onukwuli OD. Application of experimental design methodology to optimize dye removal by mucuna- sloanei induced coagulation of dye-based waste-water. Desalin Water Treat 2020;198:396–406.
[27] Anadebe VC, Onukwuli OD, Omotioma M, Okafor NA. Experimental, theoretical modeling and optimization of inhibition efficiency of *pigeon pea* leaf extract as anti-corrosion for mild steel in acid environment. Mater Chem Phys 2019;233:120–32.
[28] Anadebe VC, Onukwuli OD, Omotioma M, Okafor NA. Optimization and electrochemical study on the control of mild steel corrosion in HCl acid solution with bitter kola leaf extract as inhibitor. S Afr J Chem 2018;71:51–61.
[29] Okafor CS, Anadebe VC, Onukwuli OD. Experimental, statistical modeling and molecular dynamics simulation concept of sapium ellipticum leaf extract as corrosion inhibitor for CS in acid environment. S Afr J Chem 2019;72:164–75.
[30] Onukwuli OD, Anadebe VC, Okafor CS. Optimum prediction of inhibition efficiency of sapium ellipticum leaf extract as corrosion inhibitor of aluminum alloy (AA3003) in HCl using electrochemical impedance study and response surface method. Bull Chem Soc Ethiop 2020;34(1):175–91.
[31] Nur Izzah NH, Shafreeza S, Norazila K. Oil palm empty fruit bunch extract as green inhibitor for mild steel in hydrochloric acid solution: central composite design optimization. Mater Corros 2018:1–9.
[32] Anees AK, Mustafa SM, Hameed BM. Mathematical regression and artificial neural network for prediction of corrosion inhibition process of steel in acidic media. J Bio Tribo Corros 2020;6:92.
[33] Olawale O, Bello JO, Ogunsemi BT, Uchella UC, Oluyori AP, Oladejo NK. Optimization of chicken nail extract as corrosion inhibitor of M-steel in 2M H_2SO_4. Heliyon 2019;5:e02821.
[34] Prabhu PR, Deepa P, Padmalatha R. Analysis of *Garcinia indica Choisy* extract as friendly corrosion inhibitor for aluminum in phosphoric acid using the design of experiment. J Mater Res Technol 2020;9(3):3622–31.
[35] Anadebe VC, Okafor CS, Onukwuli OD. Electrochemical, molecular dynamics, adsorption studies and anti-corrosion activities of *Moringa leaf* biomolecules on carbon steel surface in alkaline and acid environment. Chem Data Collect 2020;28:100437.
[36] Saxena A, Prasad D, Haldhar R, Singh G, Kumar A. Use of sida cordifolia extracts as green corrosion inhibitor for mild steel in 0.5M H_2SO_4. J Environ Chem Eng 2018;6(1):694–700.
[37] El-Hamdani N, Fdil R, Tourabi MA, Jama C, Bentiss F. Alkaloids extract of retama mono- sperma (L.) Boiss. Seeds used as novel eco-friendly inhibitor for carbon steel corrosion in 1M HCl solution: electrochemical and surface studies. Appl Surf Sci 2017;357:1294–305.
[38] Saviour AU, Solomon MM, Shaikh AA, Hatim DM. Synthesis, characterization and utilization of a diallylmethylamine-based cyclopolymer for corrosion mitigation in simulated acidizing environment. Mater Sci Eng C 2019;100:897–914.

[39] Solomon MM, Saviour AU, Quraishi MA, Mohammad S. Myristic acid based imidazoline derivative as effective corrosion inhibitor for steel in 15% HCl medium. J Colloid Inter Sci 2019;551:47–60.
[40] Ehsani A, Mahjani MG, Hosseini M, Safari R, Moshrefi R, Shiri HM. Evaluation of thymus vulgaris plant extract as an eco-friendly corrosion inhibitor for stainless steel 304 in acidic solution by means of electrochemical impedance spectroscopy, electrochemical noise analysis and density functional theory. J Colloid Inter Sci 2017;480:444–51.
[41] Sanaei Z, Shahrabi T, Ramezanzadeh B. Synthesis and characterization of an effective green corrosion inhibitive hybrid pigment based on Zinc acetate-Ci- chorium intybus L leaves extract (ZnA-CIL.L): electrochemical investigations on the synergistic corrosion inhibition of mild steel in aqueous chloride solutions. Dyes Pigments 2017;139:218–32.
[42] Rose K, Byoung SK, Rajagopal K, Arumugam S, Devarayan K. Surface protection of steel in acid medium by Tabernaemontana divaricate extract: physiochemical evidence for adsorption of inhibitor. J Mol Liq 2016;214:111–6.
[43] Bahlakeh G, Ramazanzadeh M, Ramezanzadeh B. Experimental and theoretical studies of the synergistic inhibition effects between the plant leaves extract (PLE) and zinc salt (ZS) in corrosion control of carbon steel in chloride solution. J Mol Liq 2017;248:854–70.
[44] Anupama KK, Ramya K, Shainy KM, Joseph A. Adsorption and electrochemical studies of Pimenta dioica leaf extracts as corrosion inhibitor for mild steel in hydrochloric acid. Mater Chem Phys 2015;167:28–41.
[45] Ituen EK, Akaranta O, James A, Sun S. Green and sustainable local biomaterials for oilfield chemicals: griffonia simplicifolia extract as steel corrosion inhibitor in hydrochloric acid. Sustain Mater Technol 2017;11:12–8.
[46] Elmsellem H, Bendaha H, Aouniti1 A, Chetouani1 A, Mimouni M, Bouyanzer A. Comparative study of the inhibition of extracts from the peel and seeds of Citrus Aurantium against the corrosion of steel in molar HCl solution. Mor J Chem 2014;2(1):1–9.
[47] Mohammadi Z, Rahsepar M. The use of green *bistorta officinalis* extract for effective inhibition of corrosion and scale formation problems in cooling H_2O system. J Alloys Compd 2017;770:669–78.
[48] Mokhtar B, Abdelkader M, Nora B, Mahieddine N. Mild steel corrosion inhibition by parsley (petroselium sativum) extract in acidic media. Egypt J Pet 2019;28:155–9.
[49] Tan B, Zhang S, Qiang Y, Guo L, Feng L, Liao C, Xu Y, Chen S. A combined experimental and theoretical study of the inhibition effect of three disulfide-based flavoring agents for Cu corrosion in 0.5M sulfuric acid. J Colloid Interface Sci 2018;526:268–80.
[50] Gerengi H. Anticorrosive properties of date palm (*phoenix dactylifera* L.) fruit juice on 7075 type aluminum alloy in 3.5% NaCl Solution. Ind Eng Chem Res 2012;51:12835–43.
[51] Jianhong T, Lei G, Hong Y, Fan Z, El-Bakri Y. Synergistic effect of potassium iodide and sodium dodecyl sulfonate on the corrosion inhibition of carbon steel in HCl medium: a combined experimental and theoretical investigation. RSC Adv 2020;10:15163–70.
[52] Ibrahim T, Habbab M. Corrosion inhibition of mild steel in 2M HCl using aqueous extract of eggplant peel. Int J Electrochem Sci 2011;6:5357–71.
[53] Ting Y, Shengtao Z, Li F, Yujie Q, Lansi L, Denglin F, Yanan W, Jida C, Wenpo L, Bochua T. Investigation of imidazole derivatives as corrosion inhibitors of copper in sulfuric acid: combination of experimental and theoretical research. J Taiwan Inst Chem Eng 2020;106:118–29.
[54] Elmsellem H, Harit T, Aouniti A, Malek F, Riahi A, Chetouani A, Hammouti B. Adsorption properties and inhibition of mild steel corrosion in 1M HCl solution by some bipyrazolic derivatives: experimental and theoretical investigations. Protect Met Phys Chem Surf 2015;51:873–84.
[55] Solomon MM, Umoren SA. Electrochemical and gravimetric measurements of inhibition of aluminum corrosion by poly (meth acrylic acid) in H_2SO_4 solution and synergistic effect of iodide ions. Measurement 2015;76:104–16.
[56] Zou C, Yan X, Qin Y, Wang M, Liu Y. Inhibiting evaluation of β-cyclodextrin modified acrylamide polymer on alloy steel in sulfuric solution. Corros Sci 2014;201:790–803.
[57] Elmsellem H, Nacer H, Halaimia F, Aouniti A, Lakehal I, Chetouani A, Al-Deyab SS, Warad I, Touzani R, Hammouti B. Anti-corrosive properties and quantum chemical study of (E)-4-Methoxy-N-(Methoxybenzylidene) Aniline and (E)-N-(4-Methoxybenzylidene)-4-Nitroaniline coating on mild steel in molar hydrochloric. Int J Electrochem Sci 2014;9:5328–51.
[58] Elmsellem H, Basbas N, Chetouani A, Aouniti A. Quantum chemical studies and corrosion inhibitive properties of mild steel by some pyridine derivatives in 1M HCl solution. Portugal Electrochim Acta 2014;32(2):77–108.
[59] Al-Moubaraki AH. Corrosion protection of mild steel in acid solutions using red cabbage dye. Chem Eng Commun 2015;202:1069–80.
[60] Verma C, Obot IB, Bahadur I, Sherif E-SM, Ebenso EE. Choline based ionic liquids as sustainable corrosion inhibitors on mild steel surface in acidic medium: gravimetric, electrochemical, surface morphology, DFT and Monte Carlo simulation studies. Appl Surf Sci 2018;457:134–49.
[61] Zhang J, Liu Z, Han G, Chen S, Chen Z. Inhibition of copper corrosion by the formation of schiff base self-assembled monolayers. Appl Surf Sci 2016;389:601–8.
[62] Feng Y, Chen S, Guo W, Zhang Y, Liu G. Inhibition of iron corrosion by 5,10,15,20-tetraphenylporphyrin and 5,10,15,20-te- tra-(4-chlorophenyl) porphyrin adlayers in 0.5M H_2SO_4 solutions. J Electroanal Chem 2007;602:115–22.
[63] El-Faydy M, Touir R, Ebn Touhami M, Zarrouk A, Jama C, Lakhrissi B, Olasunkanmi LO, Ebenso EE, Bentiss F. Corrosion inhibition performance of newly synthesized 5- alkoxymethyl-8-hydroxyquinoline derivative for carbon steel in 1M HCl solution: experimental, DFT and Monte Carlo simulation studies. Phys Chem Chem Phys 2018;20:20167–87.
[64] Rouifia Z, Benhiba F, El-Faydy M, Laabaissi T, About H, Oudda H, Warad I, Guenbour A, Lakhrissi B, Zarrouk A. Performance and computational studies of new soluble triazole as corrosion inhibitor for carbon steel in HCl. Chem Data Collect 2019;22:100242.
[65] Keshavarzi A, Fereydoon S, Jalal S, Munawar I, Tirado-Corbalá R, El-Sayed Ewis O. Application of ANFIS-based subtractive clustering algorithm in soil cation exchange capacity estimation using soil and remotely sensed data. Measurement 2017;95:173–80.
[66] Lin C, Zhibin L, Nannan M, Yi W. Prediction of oilfield-increased production using adaptive neuro fuzzy inference system with smoothing treatment. Math Probl Eng 2019 Article ID 4865712, 11 Pages.
[67] Ekemini I, Victor M, Eno M, Obot Ime. Electrochemical kinetics, molecular dynamics, adsorption and anticorrosion behavior of melatonin biomolecule on steel surface in acid medium. Bioelectrochemistry 2019;129:42–53.
[68] Alibakhshi E, Ramezanzadeh M, Haddadi SA, Bahlakeh G, Ramezanzadeh B, Mahdavian M. Persian Liquorice extract as a highly efficient sustainable corrosion inhibitor for mild steel in sodium chloride solution. J Clean Prod 2019;210:660–72.
[69] Abderrahim K, Chouchane T, Selatnia I, Sid A, Mosset P. Evaluation of the effect of Tetramethyl ammonium hydroxide on the corrosion inhibition of A9Msteel in industrial water: an experimental, morphological and MD simulation insights. Chem Data Collect 2020;28:100391.
[70] Latifa H, Abdelhak K, Salah M, Soumia B. Corrosion inhibition of Fe-19Cr stainless steel by glutamic acid in 1M HCl. Chem Data Collect 2020;28:100455.
[71] Parook FK, Vaithianathan S, Rupesh KB, Srinivasan M, Rakesh CB. Effect of benzotriazole on corrosion inhibition of copper under flow conditions. J Environ Chem Eng 2015;3:10–9.
[72] Akhil S, Dwarika P, Rajesh H. Investigation of corrosion inhibition effect and adsorption activities of *cuscuta reflexa* extract for mild steel in 0.5M H_2SO_4. Biolelectrochemistry 2018;107:156–64.
[73] Medi TM, Ramezanzadeh M, Ramezanzadeh B, Bahlakeh G. Production of an environmentally stable anticorrosion film based on esfand seed extract molecules-metal cations: integrated experimental and computer modelling approaches. J Hazard Mater 2020;382:121029.